

## **Analysis of a Potential Hidden Geothermal System in the Granite Mountain Area of Buena Vista Valley, Pershing County, Nevada**

Ian Adams<sup>1</sup>, James E. Faulds<sup>1</sup>, Jules Grellier<sup>2</sup>, Bastien Hermant<sup>2</sup>

<sup>1</sup>Nevada Bureau of Mines and Geology, University of Nevada, Reno, NV 89557

<sup>2</sup>TLS Geothermics, 91 Chemin de Gabardie, 31500, Toulouse, FRANCE

ijadams@unr.edu

**Keywords:** Great Basin, geology, geophysics, exploration

### **ABSTRACT**

The Great Basin region of the Basin and Range province, which encompasses nearly all of Nevada and parts of Idaho, Oregon, Utah, and California, is a tectonically active region undergoing regional extension and transtension. Active faulting in the Great Basin is a key factor in creating favorable conditions for geothermal activity. The geothermal potential within the region comes with challenges of characterizing the systems, because most of the geothermal resources are blind or hidden with no surface manifestations such as hot springs. This study assesses a potential hidden geothermal system within western Nevada through integration of geological and geophysical data. The study is focused on the Granite Mountain area of Buena Vista Valley in Pershing County, Nevada, where favorable structural settings and other geothermal indicators indicate relatively high potential for hosting a geothermal system. The structural framework of the Granite Mountain-Buena Vista Valley area consists primarily of a system of west-dipping normal faults along the eastern margin of Buena Vista Valley, which includes fault intersections and step-overs (i.e., relay ramps). These structural settings can generate zones of enhanced permeability that may provide favorable pathways for geothermal fluids. Additionally, intersecting gravity gradients and low resistivity anomalies further suggest subsurface structural and hydrothermal features conducive to or indicative of geothermal activity. The combination of these structural and geophysical characteristics suggests that the area may host a hidden geothermal system. By combining multiple datasets, this study aims to identify key structural and geophysical characteristics that define prospective hidden geothermal systems in the Great Basin region. Results from this project will contribute to identifying areas for temperature gradient drilling in the Granite Mountain area and potentially help guide future exploration in the region.

### **1. INTRODUCTION**

The Great Basin region of the western United States is characterized by active extension and transtension associated with Basin and Range tectonics, which play a fundamental role in controlling geothermal potential. Regional extension has thinned the crust and lithosphere, resulting in elevated geothermal gradients relative to much of the continental United States (Coolbaugh et al., 2002, 2005; Blackwell et al., 2011). This high geothermal gradient, combined with widespread Quaternary faulting, generates favorable conditions for the development of geothermal systems, where permeability is sufficient to allow fluid circulation. In such extensional settings, the presence of favorable structural settings are commonly the primary controls on geothermal fluid flow rather than heat supply alone (e.g., Curewitz and Karson, 1997; Faulds et al., 2006; Bell and Ramelli, 2007).

Despite these favorable conditions, identifying geothermal systems in the Great Basin region remains challenging, because many resources are hidden beneath the surface and lack diagnostic surface manifestations such as hot springs or fumaroles (Richards and Blackwell, 2002; Garg et al., 2010; Craig et al., 2021). These hidden geothermal systems constitute a substantial portion of known geothermal resources in Nevada (Faulds et al., 2021a) and are thought to represent an even larger fraction of the regions undiscovered geothermal potential (Coolbaugh et al., 2007). The absence of surface indicators necessitates alternative exploration strategies that rely on structural geology, geophysics, and geochemistry among other techniques. Favorable structural settings provide an important first-order framework for targeting potential hidden geothermal systems (Faulds and Hinz, 2015). However, the abundance of such structural features throughout the Great Basin underscores the need for additional constraints to distinguish which settings are most likely to host economically viable geothermal resources.

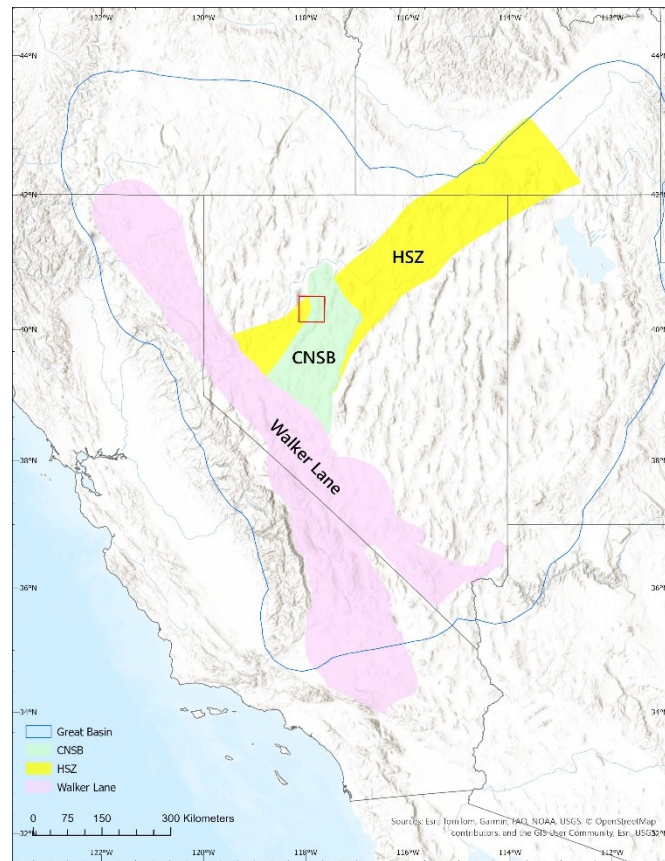


**Figure 1: Map showing Walker Lane, central Nevada seismic belt (CNSB), Humboldt structural zone (HSZ), and Great Basin. Location of figure 2 represented by the red polygon.**

Advances in geothermal exploration emphasize the importance of integrating geological, structural, and geophysical datasets to reduce uncertainty and exploration risk (e.g., Craig et al., 2021). These advances are mostly driven by both academic research and industrial players. In the case of the Granite Mountain area, TLS Geothermics, a French exploration company, has developed a conceptual approach to the geothermal exploration workflow, allowing selection of more potential hidden systems in the region, and is collaborating with the Nevada Bureau of Mines and Geology at the University of Nevada, Reno, to assess geothermal potential at specific sites in Nevada.

Regional-scale approaches, such as play fairway analysis and emerging data-driven techniques, have successfully highlighted areas of elevated geothermal favorability (Faulds et al., 2021b; Smith et al., 2023). This includes portions of Buena Vista Valley and the adjacent southern part of the East Range near Granite Mountain in Pershing County, Nevada, which was identified by the machine learning-powered prospecting tool DIG4GEO<sup>®</sup> developed by TLS Geothermics. These assessments identified Granite Mountain as a location where favorable structural settings coincide with other favorable geothermal indicators. Building on this regional context, this study focuses on the Granite Mountain area to assess the potential for a hidden geothermal system through the integration of new detailed geologic mapping, structural analysis, newly acquired shallow temperature measurements, and geophysical data, with the latter acquired and provided by TLS Geothermics. The objective is to identify key subsurface features such as fault zones, potential fluid upflows, and thermal anomalies that may control geothermal fluid circulation and to evaluate their implications for geothermal exploration in structurally complex regions of the Great Basin region.

## 2. GEOLOGIC SETTING

The study area lies within two tectonic structural domains within the Great Basin region (Figure 1). The first is the central Nevada seismic belt, a north-northeast-trending semi-continuous belt of enhanced Holocene seismicity in central Nevada that splays off the Walker Lane (Caskey et al., 2004). The Walker Lane is a belt of primarily dextral faults that accommodate ~25% of the relative motion between the Pacific and North American plates (e.g. Faulds and Henry, 2008; Hammond et al., 2009). The second is the Humboldt structural zone, a major east-northeast-trending crustal scale structural corridor in northern Nevada characterized by a dense network of faults, fractures, and lineaments that have developed through repeated episodes of tectonic deformation (Rowan and Wetlaufer, 1981). Left-lateral shear within the Humboldt structural zone may further enhance west-northwest-directed extension, compounding the structural complexity of the region (Faulds et al., 2012). These zones of enhanced extension in the active extensional to transtensional setting induce both high heat flow and dilation on normal faults generating an optimal environment for geothermal activity (Faulds et al., 2006, 2012).

The stratigraphic framework of the Granite Mountain area in the southern East Range is composed of highly deformed upper Paleozoic basin-derived metasedimentary rocks to Permo-Triassic volcanic and Triassic marine carbonate rocks intruded by both Triassic

leucogranite and Oligocene monzonite on Granite Mountain and nonconformably overlain by Oligocene to Miocene volcanic and sedimentary rocks. Miocene sedimentary rocks, rhyolite lavas, and basalt flows crop out in the lower ridges to the south of Granite Mountain and east of McKinney Pass. Quaternary alluvium and lacustrine deposits in the Buena Vista basin onlap all the older strata (Figure 2) (Muller et al., 1951; Whitebread and Sorensen, 1980; Fosdick and Colgan, 2008).

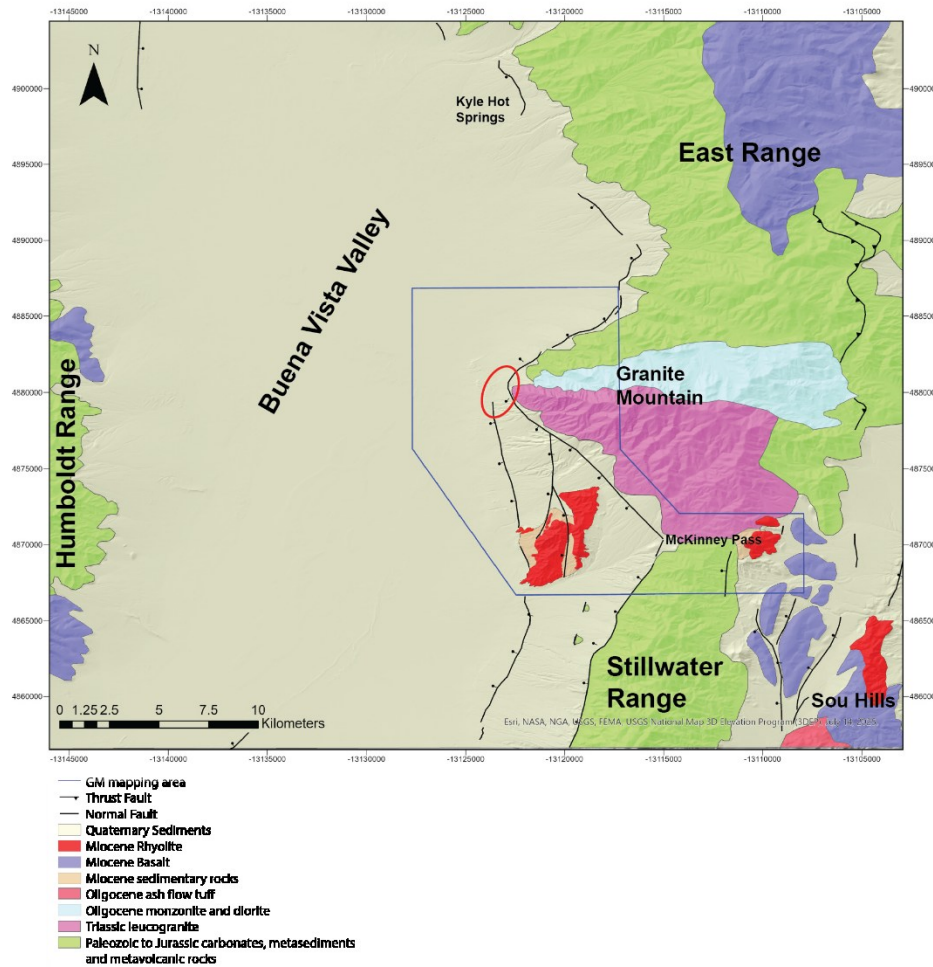


**Figure 2: Generalized geologic map of Granite Mountain area (blue polygon) and surrounding region. Red ellipse represents main step over**

The structural framework of the study area is dominated by east-tilted fault blocks bounded by major west-dipping normal faults. The Buena Vista basin is a large generally east-tilted half-graben bounded to the east by west-dipping strands of the Buena Vista Valley normal fault zone. The East Range is the uplifted block comprising the footwall of the Buena Vista fault zone. The southern East Range (including Granite Mountain) represents the exhumed footwall of this fault system and has also been tilted eastward in response to movement on the broad system of west-dipping normal faults in the region. The primary area of interest within the study area is a hybrid favorable structural setting consisting of a large right step-over and multiple fault intersections within the Quaternary normal faults across the nose of Granite Mountain.

### 3. DATA AND RESULTS

To investigate the Granite Mountain study area, detailed geological mapping, a 2-meter temperature survey, and geophysical surveys were employed.

#### 3.1 Geological Mapping and Structural Analysis

A new 1:24,000 scale geological map of the study area was prepared to elucidate the stratigraphic and structural framework of the Granite Mountain area. Approximately ~140 km<sup>2</sup> were mapped with the aid of LiDAR and NAIP imagery. Mapping across Granite Mountain indicates that faults cutting the western side of the mountain cut both the Triassic leucogranite and the Oligocene monzonite, constraining fault activity to post-Oligocene time. Quartz veins are commonly observed within fractures in the leucogranite and exploit pre-existing brittle fractures and possibly faults. These veins postdate emplacement of the Triassic host rock and may predate or be contemporaneous with Cenozoic dip-slip normal faulting, as suggested by their similar orientations to mapped faults.

Field mapping also reveals that Miocene rhyolite units exposed in the southern part of the study area are more laterally continuous to the north than previously mapped, with additional outcrops identified near the main fault step-over at the western tip of Granite Mountain (Figure 2). The northern extent of the rhyolite exhibits a higher degree of hydrothermal alteration relative to southern exposures.

LiDAR data were used to identify the locations of Quaternary faults and assess the age of most recent rupture (i.e., recency) and slip rates on such faults. The LiDAR analysis highlights a major fault system within the study area that generally strikes northerly to the south of the western tip of Granite Mountain, followed by a distinct change to a northeast strike near the western tip of the range. The northerly striking segment is referred to as the eastern Buena Vista fault zone, whereas the northeast striking segment is designated the Granite Mountain fault zone. The Granite Mountain fault accommodates approximately 10–15 m of offset of the Quaternary alluvium, compared to the eastern Buena Vista fault, which shows approximately 5 m of offset of the Quaternary alluvium. This difference in displacement suggests spatial variability in deformation, potentially reflecting differences in slip rate, fault longevity, or number of rupture events. The orientation of the Granite Mountain fault zone is roughly perpendicular to the least principal stress in the current stress field (e.g., Bennett et al., 2003), suggesting a more favorable orientation for normal slip compared to other faults in the study area.

The relative ages of Quaternary faults in the study area are primarily constrained by their relationships with Lake Lahontan deposits. Across the Buena Vista Valley fault zone, many fault traces are spatially coincident with the Lake Lahontan high stand shoreline but have not accommodated significant offset of lacustrine deposits. This relationship suggests that the latest movement on these faults predate the Lake Lahontan high stand (~12 ka) or have not experienced surface-rupturing events since that time (Reheis, 1999).

Several faults that are not visible in LiDAR but inferred from gravity data lack observable surface displacement in Lake Lahontan basin deposits. The absence of offset in sediments younger than approximately 12 ka suggests that these structures are older than the latest Lake Lahontan high stand and have not experienced surface-rupturing events in the Holocene.

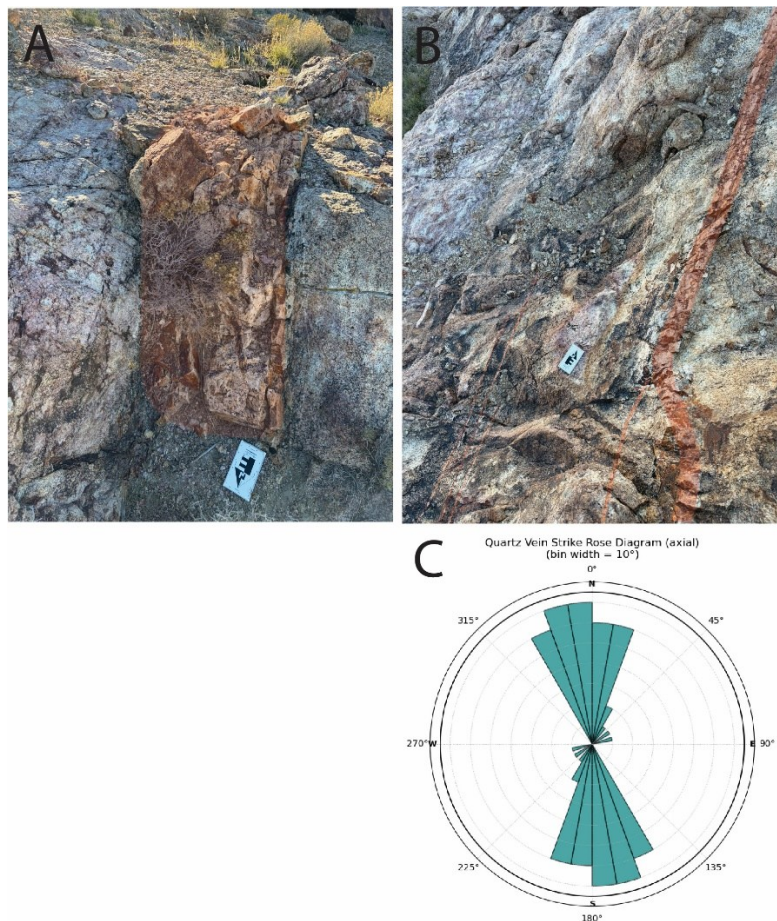


**Figure 3: A: ~1 m thick quartz vein on Granite Mountain highlighted in red. B: Quartz veins ranging from ~1-10 cm cutting through leucogranite. Highlighted in red. Top left of image shows zone of increased alteration. C: Rose diagram of strikes of quartz veins on Granite Mountain.**

These observations have revealed areas of increased structural complexity and alteration near the major fault intersection off the tip of Granite Mountain. For example, from east to west across Granite Mountain, several features become increasingly prominent. This includes: 1) an increase in joint density, 2) intensification of hydrothermal alteration, with granitic rocks becoming more iron stained and

greater alteration of feldspars to clays, 3) quartz veining becomes more pervasive, and 4) the density and thickness of quartz veins increases, with individual veins reaching up to 1 m in width near the western tip of Granite Mountain (Figure 3).

### 3.2 Two-Meter Temperature Survey

Shallow temperature or 2-m temperature surveys are a cost-effective method for evaluating a prospect for thermal anomalies that may indicate geothermal upwellings and/or outflow (Kratt et al., 2008, 2009, 2010). These surveys involve measuring ground temperatures at a depth of 2 m, which is below the zone influenced by daily solar heating, allowing for the identification of temperature anomalies that may signal geothermal resources. To account for variation within the ground surface, a base station is established to account for any background and seasonal changes (Kratt et al., 2010; Coolbaugh et al., 2014; Kraal et al., 2024).

The acquisition of 2-m temperature data at Granite Mountain consisted of gathering 53 stations across two campaigns in August and October, 2025. The points covered roughly 14 km from north to south and from the western tip of Granite Mountain on the east to the Buena Vista playa on the west. After data acquisition the 2-m temperatures were corrected for albedo and elevation and then standardized to a degree above background using the standard correction methodologies (Kraal et al., 2024). After corrections, the survey yielded an anomaly of ~3.3°C above background, which is large enough in terms of degrees above background (DAB) to be considered anomalous (Kraal et al., 2024). The anomaly, shown in Figure 4, is directly west of the nose of Granite Mountain, amid a complex set of intersecting and stepping faults. There are also two smaller anomalies to the north and south within the Granite Mountain area, but they do not meet the criteria for a standard 2-meter anomaly, which is 3.0°C DAB.

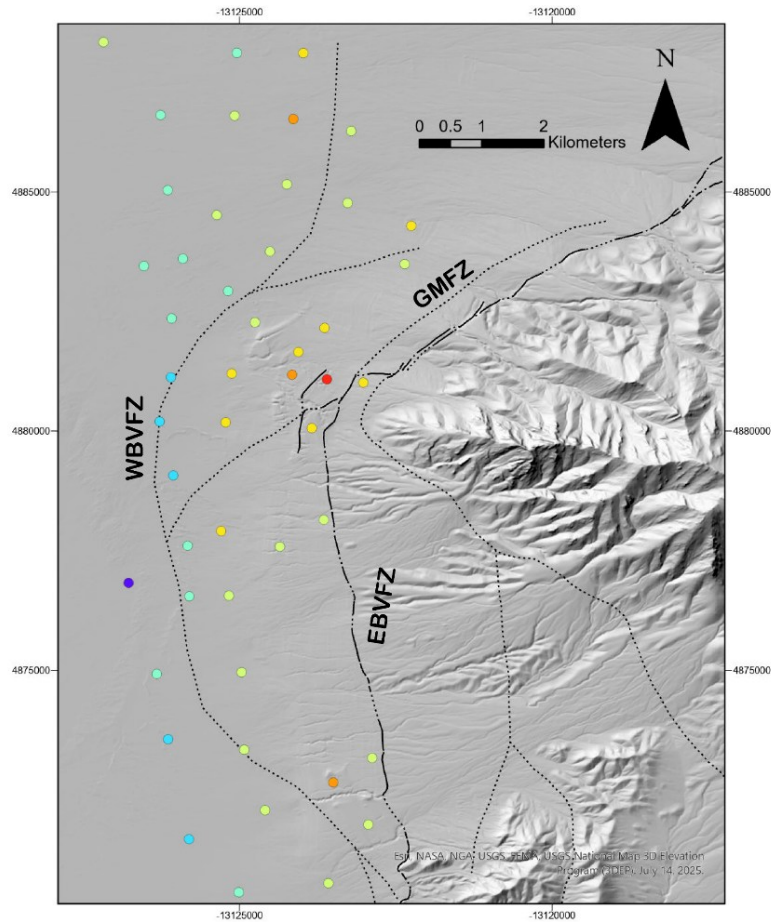


**Figure 4: 2-m temperature survey results in the Granite Mountain area in Buena Vista Valley are shown as colored circles. Quaternary faults shown from interpretation of LiDAR and geophysical (gravity and magnetics) data. Granite Mountain fault zone - GMFZ, eastern Buena Vista fault zone – EBVFZ, western Buena Vista fault zone – WBVFZ.**

### 3.3 Geophysical Surveys

Geophysical data were acquired by TLS Geothermics to help to identify intrabasinal faults, alteration zones, and potential geothermal upwellings, providing critical insights into subsurface structures and possible geothermal activity.

### 3.3.1 Gravity Data

Four hundred gravity stations were collected by Zonge International Inc. in April and June 2024, with an average station spacing of approximately 800 m across the study area. The data were reduced using a density of 2.45 g/cc and gridded at 200 m to produce the complete Bouguer anomaly (CBA). The dataset was further processed to generate the horizontal gradient magnitude (HGM) and the first vertical derivative (1VD). The horizontal gradient helps delineate sharp density boundaries, such as faults, whereas the vertical derivative enhances shallow features and aids in estimating depth to sources (Blakey, 1996).

The gravity data permit many interpretations about the structure of the Granite Mountain field area. The HGM (Figure 5B) shows the highest density contrast across the entire study area along a northerly trend (western Buena Vista fault) extending to the nose of Granite Mountain, where it bifurcates into both north and northeast segments. The northeast-trending gradient aligns with the previously mentioned Granite Mountain fault zone. In contrast, the eastern Buena Vista fault does not exhibit a distinct expression in the HGM data; however, its intersection with the Granite Mountain fault zone near the nose of Granite Mountain coincides with anomalous points identified in the 2-m temperature survey.

The 1VD of the gravity suggests a denser body just to the east of the western Buena Vista fault. This pattern may reflect tilting of the range-bounding fault along the East Range to a lower dip causing a shallower depth to basement in the area (Fosdick and Colgan, 2006). In contrast, the western Buena Vista fault appears to dip more steeply, producing greater stratigraphic offset. This larger displacement likely generates the pronounced gravity contrast observed across the basin and implies a shallower depth to basement east of the western Buena Vista fault.

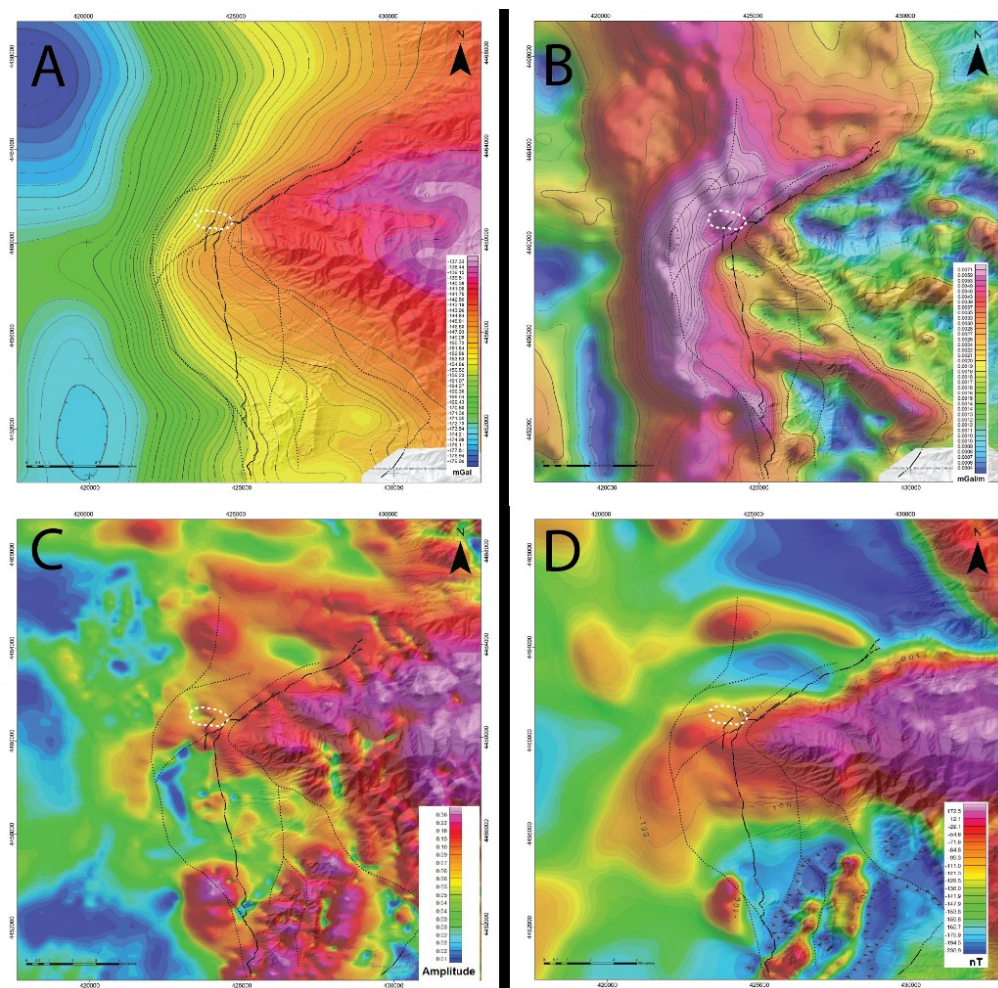


**Figure 5: Gravity and magnetic survey results. White polygon represents the 2-m temperature anomaly. A: CBA reduced at 2.45 g/cc. B: Horizontal gradient magnitude (HGM) of the CBA. C: Analytic signal from total magnetic intensity data. D: Reduced to pole (RTP) magnetic anomaly. Quaternary faults shown from interpretation of LiDAR and geophysical (gravity and magnetics) data.**

### 3.3.2 Magnetic Data

Airborne magnetic data were acquired as part of the GeoDAWN project, a collaborative effort between the U.S. Geological Survey (USGS) and the U.S. Department of Energy (DOE) to collect high-resolution airborne magnetic data across the western Great Basin (Glen

and Earney, 2023). These data can be used to identify geological structures such as faults and to delineate zones of enhanced hydrothermal alteration, where magnetite destruction reduces the overall magnetization of the host rocks (Bouligand et al., 2014).

Analytic signal processing of the magnetic data highlights strong lateral gradients in magnetization (Roest et al., 1992), with a pronounced magnetic body observed east of the western Buena Vista fault zone identified in the horizontal gradient magnitude (HGM) of the gravity data (Figure 5). The correspondence of elevated magnetic response and gravity gradients suggests a shallower magnetic basement east of the western Buena Vista fault. This interpretation is consistent with structural juxtaposition across the fault, where higher-density and more magnetic basement rocks are inferred to be much closer to the surface on the eastern side of the fault.

### 3.3.3 Magnetotelluric Data

Magnetotelluric (MT) surveys are another geophysical method that can aid in the exploration of geothermal prospects. It is a powerful tool for geothermal resource assessment, because the presence of high-temperature saline fluids and associated clay alteration zones typically exhibit pronounced conductive signatures (e.g., Cagniard, 1953; Cumming, 2009; Wannamaker et al., 2017).

A total of 78 MT stations were collected across the study area and subsequently processed and inverted to create a 3D resistivity model of the Granite Mountain area. This comprehensive model gives good insight into the subsurface and highlights different potential zones of increased alteration.

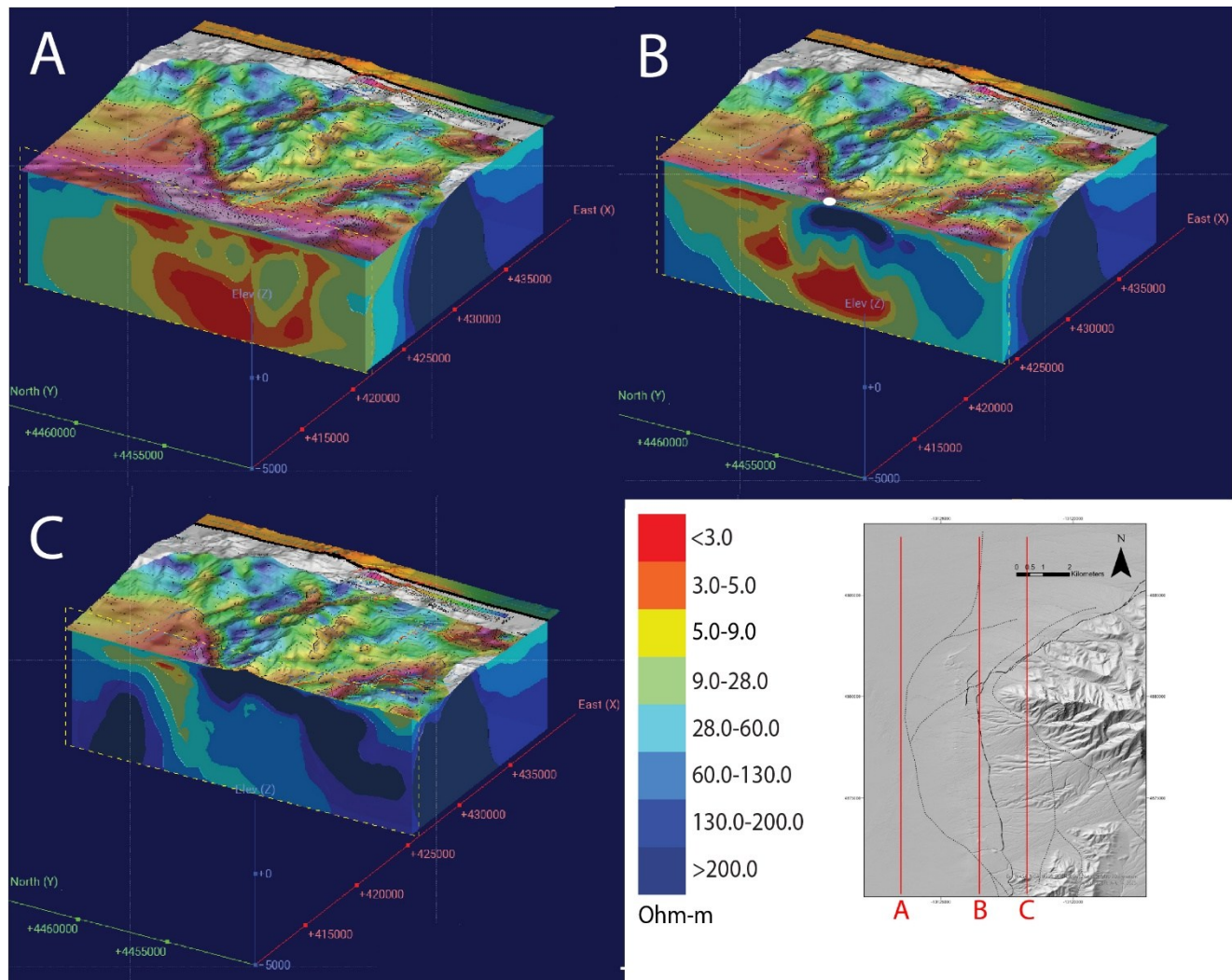


**Figure 6: Slices through the 3D MT model in cross section view, with HGM of the gravity draped over topography. The locations of the cross sections are indicated by red lines on the map view. White ellipse shows 2-m anomaly location. Scale in Ohm-m**

The cross-sectional slices presented in figure 6 demonstrate how the subsurface resistivity changes when crossing the complex fault intersection within the Granite Mountain area. As the profiles cross the main faults shown by the HGM draped over the MT, there is a clear low resistive body on the west side of the western Buena Vista fault with resistive bodies on the east side. This juxtaposition of

resistivity correlates with the density contrast observed in the gravity data (Figure 5). The CBA gravity exhibits a higher gravity signal on the east side relative to the west in the same location.

Figure 6b shows the 2-m temperature anomaly where the low resistive body pinches out around the anomaly. Figure 6c illustrates that the conductive structure begins to dissipate with that trend continuing to the northeast out of the area with great structural complexity. Overall, the MT data provide evidence of a large conductive body along the main fault zone of the Granite Mountain study area.

#### 4. DISCUSSION

Detailed geological mapping, structural analysis, a 2-m temperature survey, and geophysical surveys were employed to evaluate the potential for a hidden geothermal system in the Granite Mountain area along the eastern margin of Buena Vista Valley. Collectively, these datasets indicate that a complex favorable structural setting for geothermal activity, including both fault intersections and a step-over, occupies the westernmost part of Granite Mountain and adjacent parts of Buena Vista Valley. The systematic increase in hydrothermal alteration and joint density toward the western nose of Granite Mountain suggests that this area may have provided a zone of enhanced permeability, facilitating fluid circulation. Increased joint density and intersecting faults likely provided interconnected pathways for hydrothermal fluids, potentially forming a highly fractured geothermal reservoir, as evidenced by relatively abundant quartz veins exposed in the mutual footwall of the intersecting faults (Figure 3).

Although no surface geothermal manifestations (e.g., hot springs or steam vents) are found in the area, the preserved alteration assemblages and vein networks in the footwall of the Buena Vista fault zone proximal to the subtle 2-m anomaly in the adjacent hanging wall (Figure 4) indicate that the area was once influenced by a hydrothermal system and that system may still be active. The westward intensification of alteration may further suggest that this system was more active near the nose of Granite Mountain, possibly resulting from the complex fault intersection in that area. Although the age of the quartz veins at Granite Mountain can only be constrained as post-Triassic, the increase in abundance toward the complex intersection of Quaternary faults at the nose of Granite Mountain and northerly strikes (Figure 3) (roughly orthogonal to the least principal stress in the current stress field) suggest a Neogene age.

We conclude that the most likely location for an active geothermal upwelling lies approximately 1 km northwest of the nose of Granite Mountain in the vicinity of the major right step-over and multiple fault intersections within Quaternary normal faults, corresponding with the primary 2-m temperature anomaly and several geophysical anomalies (Figure 5). Geophysical observations further support this interpretation. Gravity data reveal sharp density contrasts and fault geometries that bend in the area. MT results show a conductive body aligned with the western Buena Vista fault and Granite Mountain fault, interpreted as altered clays or fluid saturated materials. The pinching and dissipation of this conductive body near the 2-m temperature anomaly suggests a possible localized upflow zone. Together, structural, gravity, MT, and temperature data indicate a potential fault-controlled system in which permeability is highest in this zone of discrete fault intersections and step-overs.

#### 5. CONCLUSION

The Granite Mountain study provides an example of an integrated geological and geophysical approach to evaluating a potential hidden geothermal system in the Great Basin region. Work completed to date has advanced the prospect from an area identified through play fairway and favorability analyses to a more constrained model supported by geological mapping, shallow temperature measurements, and detailed geophysical surveys. Structural analysis highlights fault intersections and a major step-over proximal to the western nose of Granite Mountain as key zones of enhanced permeability, while a 2-m temperature anomaly and corresponding gravity and MT anomalies suggest elevated geothermal potential. Although additional work is required to confirm the presence of an active, power capable resource, the results identify a compelling target for future drilling. Continued development of a conceptual model through additional data acquisitions and modeling will help guide future exploration and reduce uncertainty in the assessment of hidden geothermal systems in the region.

## REFERENCES

- Bell, J.W., and Ramelli, A.R., 2007, Active faults and neotectonics at geothermal sites in the western Basin and Range: Preliminary results: *Geothermal Resources Council Transactions*, v. 31, p. 375–379.
- Bennett, R.A., Wernicke, B.P., Niemi, N.A., Friedrich, A.M., and Davis, J.L., 2003, Contemporary strain rates in the northern Basin and Range province from GPS data: *Tectonics*, v. 22, p. 1-31, doi:10.1029/2001TC001355.
- Blackwell, D.D., Richards, M., Frone, Z., and Batir, J., 2011, Temperature-at-depth maps for the conterminous U.S. and geothermal resource estimates: *Geothermal Resources Council Transactions*, v. 35, p. 1545–1550.
- Blakely, R.J., 1996, *Potential theory in gravity and magnetic applications*: Cambridge University Press, 464 p.
- Bouligand, C., Glen, J.M.G., and Blakely, R.J., 2014, Distribution of buried hydrothermal alteration deduced from high-resolution magnetic surveys in Yellowstone National Park: *Journal of Geophysical Research*, v. 119, p. 2595–2630. Doi:10.1002/2013JB010802.
- Cagniard, L., 1953, Basic theory of the magnetotelluric method of geophysical prospecting: *Geophysics*, v. 18, p. 605–635, <https://doi.org/10.1190/1.1437915>.
- Caskey, S.J., Bell, J.W., Ramelli, A.R., and Wesnousky, S.G., 2004, Historic surface faulting and paleoseismicity in the area of the 1954 Rainbow Mountain–Stillwater earthquake sequence, central Nevada: *Bulletin of the Seismological Society of America*, v. 94, no. 4, p. 1255–1275, <https://doi.org/10.1785/012003012>.
- Coolbaugh, M.F., Taranik, J.V., Raines, G., Shevenell, A., Sawatzky, D., Bedell, R., and Minor, T.B., 2002, A geothermal GIS for Nevada: Defining regional controls and favorable exploration terrains for extensional geothermal systems: *Geothermal Resources Council Transactions*, p. 485–490.
- Coolbaugh, M., Sladek, C., Faulds, J., Zehner, R., and Oppliger, G., 2007, Use of rapid temperature measurements at a 2-meter depth to augment deeper temperature gradient drilling: *Stanford Geothermal Reservoir Engineering Workshop*.
- Coolbaugh, M., Zehner, R., Kreemer, C., Blackwell, D., and Oppliger, G., 2005, A map of geothermal potential for the Great Basin, USA: Recognition of multiple geothermal environments: *Geothermal Resources Council Transactions*, v. 29, p. 223–228.
- Coolbaugh, M., Zehner, R., and Kratt, C., 2014, Shallow temperature surveys for geothermal exploration in the Great Basin, USA, and estimation of shallow aquifer heat loss: *Geothermal Resources Council Transactions*, v. 38, p. 115–122.
- Craig, J.W., Faulds, J.E., Hinz, N.H., Earney, T.E., Schermerhorn, W.D., Siler, D.L., Glen, J.M., Peacock, J., Coolbaugh, M.F., and Deoreo, S.B., 2021, Discovery and analysis of a blind geothermal system in southeastern Gabbs Valley, western Nevada, USA: *Geothermics*, v. 97, p. 102–177, <https://doi.org/10.1016/j.geothermics.2021.102177>.
- Cumming, W., 2009. Geothermal resource conceptual models using surface exploration data. In: *Proceedings: 34th Workshop on Geothermal Reservoir Engineering*. Stanford University, Stanford, California, 6 p.
- Curewitz, D., and Karson, J.A., 1997, Structural settings of hydrothermal outflow: Fracture permeability maintained by fault propagation and interaction: *Journal of Volcanology and Geothermal Research*, v. 79, p. 149–168, [https://doi.org/10.1016/S0377-0273\(97\)00027-9](https://doi.org/10.1016/S0377-0273(97)00027-9).
- Faulds, J.E., Coolbaugh, M., Vice, G.S., and Edwards, M.L., 2006, Characterizing structural controls of geothermal fields in the northwestern Great Basin: A progress report: *Geothermal Resources Council Transactions*, v. 30, p. 69–76.
- Faulds, J.E., Hinz, N.H., Kreemer, C., and Coolbaugh, M., 2012, Regional patterns of geothermal activity in the Great Basin region, western USA: Correlation with strain rates: *Geothermal Resources Council Transactions*, v. 36, p. 897–902.
- Faulds, J.E., and Hinz, N.H., 2015, Favorable tectonic and structural settings of geothermal systems in the Great Basin region, western USA: Proxies for discovering blind geothermal systems: *Proceedings of World Geothermal Congress, Melbourne, Australia*, 6 p.
- Faulds, J.E., Coolbaugh, M.F., and Hinz, N.H., 2021a, Inventory of structural settings for active geothermal systems and late Miocene (~8 ma) to Quaternary epithermal mineral deposits in the Basin and Range province of Nevada: *Nevada Bureau of Mines and Geology Report 58*, 28 p.
- Faulds, J.E., Hinz, N.H., Coolbaugh, M.F., Craig, J.W., Glen, J.M., Ayling, B.F., Sadowski, A.J., Siler, D.L., and DeOreo, S., 2021b, The Nevada geothermal play fairway project: Exploring for blind geothermal systems through integrated geological, geochemical, and geophysical analyses: *Proceedings World Geothermal Congress 2021, Reykjavik, Iceland*, 12 p.
- Fosdick, J.C., 2006, Miocene extension in the East Range, Nevada: A two-stage history of normal faulting in the northern Basin and Range [M.S. thesis]: *Stanford University*, 150 p.
- Fosdick, J.C., and Colgan, J.P., 2008, Miocene extension in the East Range, Nevada: A two-stage history of normal faulting in the northern Basin and Range: *Geological Society of America Bulletin*, v. 120, p. 1198–1213, <https://doi.org/10.1130/B26201.1>.

- Garg, S.K., Pritchett, J.W., and Combs, J., 2010, Exploring for hidden geothermal systems: Proceedings of the World Geothermal Conference, Bali, Indonesia, 7 p.
- Glen, J.M.G., and Earney, T.E., 2023, New high resolution airborne geophysical surveys in Nevada and California for geothermal and mineral resource studies: Geothermal Resources Council Transactions, v. 47, p. 1738–1762.
- Hinze, W.J., von Frese, R.R.B., and Saad, A.H., 2013, Gravity and Magnetic Exploration: Principles, Practices, and Applications: Cambridge, UK, Cambridge University Press, 512 p., <https://doi.org/10.1017/CBO9780511843129>.
- Kraal, K.O., Lindsey, C., Zimmerman, J., Sladek, C., and Burgess, Q., 2024, Development of shallow (2-m) temperature survey standard operating procedures and interpretation workbook: Proceedings, 49th Workshop on Geothermal Reservoir Engineering, Stanford University, SGPTR-227.
- Kratt, C., Coolbaugh, M., Sladek, C., Zehner, R., Penfield, R., and Delwiche, B., 2008, A new gold pan for the west: Discovering blind geothermal systems with shallow temperature surveys: Geothermal Resources Council Transactions, v. 32, p. 153–158.
- Kratt, C., Coolbaugh, M., Peppin, B., and Sladek, C., 2009, Identification of a new blind geothermal system with hyperspectral remote sensing and shallow temperature measurements at Columbus Salt Marsh, Esmeralda County, Nevada: Geothermal Resources Council Transactions, v. 33, p. 481–485.
- Kratt, C., Sladek, C., and Coolbaugh, M., 2010, Boom and bust with the latest 2m temperature surveys: Dead Horse Wells, Hawthorne Army Depot, Terraced Hills, and other areas in Nevada: Geothermal Resources Council Transactions, v. 34, p. 567–574
- Muller, S.W., Ferguson, H.G., and Roberts, R.J., 1951, Geology of the Mount Tobin quadrangle, Nevada: U.S. Geological Survey Geologic Quadrangle Map GQ-7, scale 1:125,000.
- Reheis, M., 1999, Highest Pluvial-Lake Shorelines and Pleistocene Climate of the Western Great Basin: Quaternary Research, v. 52, p. 196–205
- Richards, M., and Blackwell, D., 2002, A difficult search: Why Basin and Range systems are hard to find: Geothermal Resources Council Bulletin, v. 31, p. 143–146.
- Roest, W.R., Verhoef, J., and Pilkington, M., 1992, Magnetic interpretation using the 3-D analytic signal: *Geophysics*, v. 57, no. 1, p. 116–125, <https://doi.org/10.1190/1.1443174>
- Rowan, L.C., and Wetlaufer, P.H., 1981, Relation between regional lineament systems and structural zones in Nevada: AAPG Bulletin, v. 65, p. 1414–1432, <https://doi.org/10.1306/03B5955D-16D1-11D7-8645000102C1865D>.
- Smith, C.M., Faulds, J.E., Brown, S., Coolbaugh, M., DeAngelo, J., Glen, J.M., Burns, E., Siler, D.L., Treitel, S., Mlawsky, E., Fehler, M., Gu, C., and Ayling, B.F., 2023, Exploratory analysis of machine learning techniques in the Nevada geothermal play fairway analysis: *Geothermics*, v. 111, <https://doi.org/10.1016/j.geothermics.2023.102693>
- Telford, W.M., Geldart, L.P., and Sheriff, R.E., 1990, Applied Geophysics, 2nd ed.: Cambridge, UK, Cambridge University Press, 770 p. <https://doi.org/10.1017/CBO9781139167932>
- Wannamaker, P.E., Moore, J.N., Pankow, K.L., and Simmons, S.D., 2017, Phase II of Play Fairway Analysis for the Eastern Great Basin Extensional Regime, Utah: Status of Indications: Geothermal Resources Council Transactions, v. 41, p. 2368–2382.
- Whitebread, D.H., and Sorensen, M.L., 1980, Preliminary geologic map of the Granite Mountain quadrangle (SE 1/4 Kyle Hot Springs quadrangle), Pershing County, Nevada: U.S. Geological Survey Open-File Report 80-715, <https://doi.org/10.3133/ofr80715>.